Generating Triaxial Reinforced Epoxy/Montmorillonite Nanocomposites with Uniaxial Magnetic Fields

Hilmar Koerner

University of Dayton Research Institute, Dayton, Ohio 45469

Edwin Hampton and Derrick Dean

Tuskegee University, Tuskegee, Alabama 36088

Zafer Turgut

UES Inc., Dayton, Ohio 45432

Lawrence Drummy, Peter Mirau, and Richard Vaia*

Air Force Research Laboratory, Materials and Manufacturing Directorate, WPAFB, Ohio 45433

Received October 23, 2004. Revised Manuscript Received February 14, 2005

The next step forward, transforming polymer nanocomposites from filled-polymer replacements to designed and engineered materials, necessitates the development of techniques to transform the random or ill-defined nanoscale morphologies into compositionally and spatially engineered hierarchal structures, paralleling that which underpins conventional continuous-fiber-reinforced composites. By exploiting an orthogonal magnetic susceptibility of montmorillonites (MMTs) from different deposits, a three-dimensional morphology composed of orthogonal alignment of aluminosilicate layers is generated from a mixture of montmorillonites and a uniaxial external magnetic field. Depending on the source, MMTs exhibit remnant magnetization arising from antiferro- and ferrimagnetic impurities and align with layers parallel or perpendicular to the field. Within a few minutes, application of static magnetic fields (1.2 or 11.7 T) induces stable alignment of organically modified MMT within an epoxy resin at room temperature. Structural relaxation is orders of magnitude slower, enabling the alignment to be captured during the subsequent cure. Thermal mechanical measurements demonstrate that morphology manipulation impacts the coefficient of thermal expansion (CTE), decreasing CTE the most in the direction of maximum MMT alignment. Knowledge of the detailed mechanism that leads to a change of the magnetic easy axis within layered silicates opens up opportunities to design novel synthetic layered silicates with unusual magnetic properties.

The term "nanocomposite" implicates parallels to traditional fiber-reinforced composite technology and the ability to spatially "engineer, design, and tailor" materials performance for a given application. The complex interrelation among nanoelements, interfacial modifiers, matrix polymers, and processing is challenging to unravel, and improvements in chemical functionalization and processing procedures are at many times system specific.[1,2] Thus, simply disrupting the low-dimensional crystallites (tactoids and ropes) to achieve a stable, uniform, quantitatively characterized distribution of the nanoelements (layered silicates and single-wall carbon nanotubes) is currently the dominating objective. But this will still lead to nanofilled polymers, not necessarily nanocomposites.

Recent mechanical modeling studies on nanofilled systems predict substantial improvements in mechanical, barrier, electrical, and thermal properties[3−8] over random dispersions if spatial control of the alignment and distribution of the nanoparticles can be achieved—emphasizing the importance of morphology manipulation down to the nanoscale. For example, Gusev et al. showed that comparable shear moduli could be obtained at only half the volume fraction of particles from a weblike morphology compared to a random or hexagonal arrangement.[5] Additional work by Gusev and coworkers on barrier properties and the coefficient of thermal expansion (CTE),[6] by Boyce et al.[3] and Balasz et al.[7] on reinforcement, and by Kumar et al. on fiber tensile strength[8] further points to the importance of nanoparticle arrangement in achieving the maximum effect at a minimum filler loading. In general, precise morphology control is paramount for optimization of electrical, thermal, and optical properties for high-tech applications, such as dielectric underfills for

(1) Alexandre, M.; Dubois, P. *Mater. Sci. Eng.* **2000**, *28*, 1.
(2) Ray, S. S.; Okamoto, M. *Prog. Polym. Sci.* **2003**, *2*, 1539.
(3) Sheng, N.; Boyce, M. C.; Parks, D. M.; Rutledge, G. C.; Abes, J. I.; Cohen, R. E. *Polymer* **2004**, *45*, 487.
(4) Gusev, A. A.; Lusti, H. R.; Hine, P. J. *Adv. Eng. Mater.* **2002**, *4/12*, 927.
(5) Gusev, A. A.; Rozman, M. G. *Comput. Theor. Polym. Sci.* **1999**, *9*, 335.
(6) Gusev, A. A.; Lusti, H. R. *Adv. Mater.* **2001**, *13*, 1641.
(7) Buxton, G. A.; Balazs, A. C. *J. Chem. Phys.* **2002**, *117* (16), 7649.
(8) Liu, T.; Kumar, S. *Nano Lett.* **2003**, *3/5*, 647.

10.1021/cm048139m CCC: $30.25
Published on Web 03/15/2005

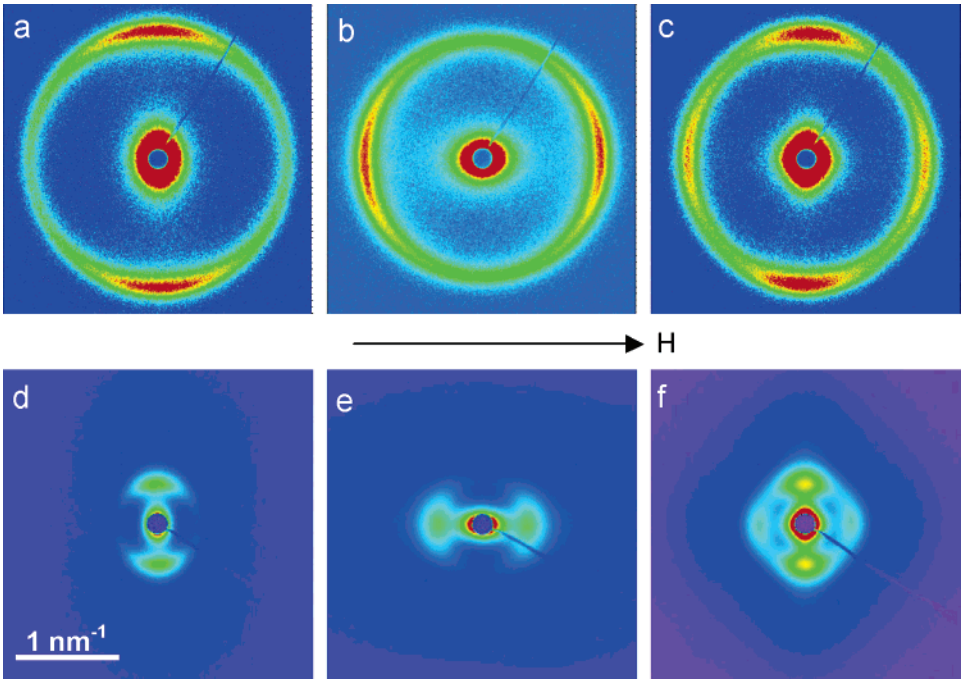

Figure 1. Small-angle X-ray scattering (SAXS) of organically modified montmorillonite (OMM) suspensions in a magnetic field (a−c, 1.2 T; d−f, 11.7 T): (a−c) X-ray of OMM suspensions without curing agent; (a) 6 wt % SC18/Epon 862 with meridional reflection at 3.48 nm; (b) 6 wt % NC18/Epon 862 with equatorial reflection at 3.78 nm; (c) 6 wt % SC18/NC18/Epon 862; (d−f) fully cured, magnetically aligned montmorillonite/epoxy nanocomposites; (d) SC18 with diffraction peak at 11.0 nm and $S_d = 0.58$; (e) NC18 with diffraction peak at 10.0 nm and $S_d = -0.26$; (f) mixture of SC18 and NC18 with diffraction peaks at 11.0 and 10.0 nm. Montmorillonites modified with primary alkylammoniums tend to substantial interlayer swelling during curing with amines, and the (001) reflection disappears from conventional wide-angle X-ray scattering, necessitating the use of SAXS. In the final nanocomposite, SAXS shows a weak correlation of OMM layers in tactoids with a broad spread of *d* spacings between 9 and 15 nm.

electronic packaging, engineered aerospace structural components, reconfigurable conductive adhesives, and optical gratings.

The ability to uniaxially align nanoelements, both plates and tubes, has been extensively demonstrated. Approaches include sedimentation, spin coating, mechanical deformation (fiber spinning, extensional deformation, extrusion, shear), magnetic fields,[9] and electrical gradients.[10,11] However, these approaches have challenges including inadequate understanding of deformation−structure correlations as well as limitations to the maximum extent of uniaxial alignment and to the maximum volume of affected material. Much less has been developed toward robust processing techniques that enable broad tunability of two- or three-dimensional structures within the bulk, and not just thermodynamic equilibrium structures such as arise from self-assembly[12] or backfilling of sacrificial templates. A successful example is holography, where directed nanoparticle distribution on the meso (100 nm) scale has been demonstrated.[13−15] Creation of complex multidimensional structures is challenged by how to controllably generate a multidimensional, morphology-directing potential within the bulk material.

Herein we discuss an alternative approach to creating three-dimensional structures using an external, uniaxial morphology-directing potential through the use of mixtures of nanoparticles with orthogonal responsivity to the external field. Specifically, montmorillonites (MMTs) from different geological deposits are chosen such that they exhibit orthogonal magnetic susceptibility with respect to the normal of the aluminosilicate sheet. Mixing powders of correctly functionalized MMTs results in triaxial reinforcement of a thermoset matrix by the aluminosilicate layers.

Figure 1 summarizes the impact of the application of a magnetic field (a−c, 1.2 T rare-earth magnet; d−f, 11.7 T NMR magnet, Oxford Instruments, Oxford, U.K.) prior to and during an initial precuring step (90 °C for 12 h) for epoxy (Epon 862/W) nanocomposites containing a 6 wt % concentration of a Nanocor (PGV, 144 mequiv/100 g) and a Southern Clay MMT (Cloisite NA, 92 mequiv/100 g) exchanged with octadecylammonium halides (NC18 and SC18, respectively). Details of the surface functionalization[16] and cure history for the Epon 862/W system are discussed in prior publications;[17] those specific to these studies are summarized along with small-angle X-ray scattering (SAXS) procedures in the Experimental Section. As initially demonstrated by Pinnavaia and co-workers[18,19] primary am-

(9) Fischer, J. E.; Zhou, W.; Vavro, J.; Llaguno, M. C.; Guthy, C.; Haggenmueller, R.; Casavant, M. J.; Walters, D. E.; Smalley, R. E. *J. Appl. Phys.* **2003**, *93* (4), 2157.
(10) Koerner, H.; Jacobs, J. D.; Tomlin, D. W.; Busbee, J.; Vaia, R. A. *Adv. Mater.* **2004**, *16*, 297.
(11) Velev, O. D. In *Encyclopedia of Nanoscience and Nanotechnology*; Schwartz, J. A., Contescu, C., Putyera, K., Eds.; Marcel Dekker: New York, 2004; pp 1025−1042.
(12) Ober, C. K. *Science* **2002**, *296*, 859.
(13) Vaia, R. A.; Dennis, C. L.; Natarajan, L. V.; Tondigila, V. P.; Tomlin, D. W.; Bunning, T. J. *Adv. Mater.* **2001**, *13*, 1570.
(14) Jakubiak, R.; Brown, D. P.; Vatansever, F.; Tondiglia, V. P.; Natarajan, L. V.; Tomlin, D. W.; Bunning, T. J.; Vaia, R. A. *Proc. SPIE* **2003**, *4991*, 89.
(15) Suzuki, N.; Tomita, Y.; Kojima, T. *Appl. Phys. Lett.* **2002**, *81* (22), 4121.
(16) Vaia, R. A.; Teukolsky, R. K.; et al. *Chem. Mater.* **1994**, *6* (7), 1017.
(17) Chen, C.; Curliss, D. *SAMPE J.* **2001**, *37/5*, 11.
(18) Pinnavaia, T. J.; Lan, T. *Proc. Am. Soc. Compos., Tech. Conf.* **1996**, *11th*, 558.
(19) Lan, T.; Pinnavaia, T. J. *Mater. Res. Soc. Symp. Proc.* **1996**, *435*, 79.

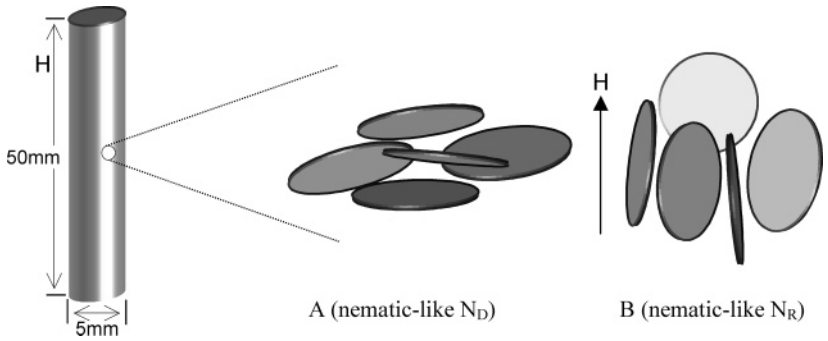

Figure 2. Schematic depiction of the resultant macroscopic uniaxial morphology for alignment of the MMT (uniaxial plate nanoparticle) with the principal axis parallel to (A, NC18) and perpendicular to (B, SC18) the magnetic field. For the present study, the plate represents stacks of correlated aluminosilicate layers.

monium modifiers result in extensive interlayer swelling during curing of bisphenol-based epoxies with amines. The slight acidity of the primary ammonium modifier leads to preferential acceleration of intergallery, relative to extragallery, cross-linking reactions. Initially the gallery height with Epon 862 (and Epon 862/W before curing (not shown)) is ~2.5 nm for both MMTs (d_{001} − 0.98 nm aluminosilicate layer thickness)—approximately consistent with the full extension of the octadecylammonium (~2.4 nm) as discussed for previous models.[20,21] The layer repeat distance increases to 11.0 nm for SC18 and 10.0 nm for NC18 after curing, while the (020) and (110) intralayer reflections at 0.448 nm remain unchanged (WAXS not shown). The final gallery height depends to a minor degree on the thermal history of the cure. For example, the layer spacing for the Epon 862/W/NC18 noted above was obtained with the following cure cycle: 12 h at 90 °C, 2 h at 120 °C, and 2 h at 180 °C. Skipping the initial precuring step at 90 °C increases the layer spacing from 10 to 12.5 nm. This reflects a tradeoff between intra- and extragallery reaction rates and the subsequent impact on monomer flow between the layers driving expansion and matrix gelation inhibiting expansion.

It is striking that the uniaxial alignment of the layers in NC18 (Herman's orientation parameter $S_d = -0.26$) is orthogonal to the magnetic field direction while the alignment created with SC18 ($S_d = 0.58$) is parallel to the magnetic field direction. This occurs in both the uncured (Figure 1b) and fully cured (Figure 1e) states. For reference, a random alignment will exhibit an orientation parameter $S_d = 0$, a completely parallel alignment, $S_d = 1$, and a completely perpendicular alignment, $S_d = -0.5$. Orientation parameters observed here are common for nematic liquid crystals. Figure 2 schematically depicts the resultant layer alignment. In these systems, the aluminosilicate layers still retain their local spatial correlation; thus, the intensity distribution of the basal reflection echoes the relative orientation of a collection of layers (swollen tactoid) with respect to the normal of the layers. An ideal, flat circular layer or a columnar collection of such layers exhibits $D_{\infty h}$ symmetry with the principal axis parallel to the layer normal. The resultant orthogonal orientation of this uniaxial nanoelement (NC18 and SC18 layers/tactoids) within the macroscopic uniaxial structure implies that each structure is unique and cannot be superimposed by a symmetry operation. Analogous to discotic and lyotropic liquid crystals, macroscopic alignment of the principal axis of the mesogen results in a discotic nematic (N_D) or alternatively a lamellar mesophase. This is the case for NC18. In contrast global alignment of the mesogens along any axis orthogonal to the principal axis of the layer does not create a common orientation direction of the principal axis. Topologically, this is analogous to a nematic collection of rods where the longest dimension of the mesogen is parallel to the uniaxial alignment direction. This is the case for SC18. The structure created by SC18, as well as the extent of alignment ($S_d \approx 0.6$), is the same as achieved by electric field processing,[10] but throughout a bulk monolith rather than a film. Note that a comparison to liquid crystals is made merely to illustrate analogies between well-known long-range orientational and short-range positional order of liquid crystals and their similarities to layered silicate nanocomposites in this study. A detailed discussion of this topic has been carried out by several other authors.[22]

The time for complete alignment of the montmorillonite depends on the viscosity of the medium and concentration of MMT, but in general, saturation is obtained after about 10 min at room temperature for 1.2 T (see the Supporting Information). On the other hand, the rate of recovery (randomization of alignment) is substantially slower. Once the suspensions have been aligned, more than 12 h is required at room temperature to randomize the tactoids. This leads to the ability to align a nanocomposite suspension and then vitrify the orientation without the presence of the external field. Slow relaxation dynamics of aligned layered silicate morphologies driven by thermal fluctuations have been previously observed,[10,23,24] and discussed with regard to frustration generated by particle−particle interactions and chain bridging. For the epoxy systems examined here, the oligomeric nature of the resin implies that the slow relaxation dynamics is governed by particle−particle interactions.

Additional experiments summarized in Table 1 with sodium-exchanged and various quaternary- and primary-alkyl-exchanged MMTs in numerous media (water, toluene, Epon 862, and Epon 828) demonstrate the universality of the response of the original MMT, irrespective of the

(20) Vaia, R. A.; Giannelis, E. P. *Macromolecules* **1997**, *30*, 7990.
(21) Vaia, R. A.; Giannelis, E. P. *Macromolecules* **1997**, *30*, 8000.
(22) Davidson, P.; Gabriel, J.-C. P. *Adv. Mater.* **2000**, *12*, 9.
(23) Ren, J.; Silver, A. S.; Krishnamoorti, R. *Macromolecules* **2000**, *33*, 3739.
(24) Schmidt, G.; Nakatani, A. I.; Butler, P. D.; Han, C. C. *Macromolecules* **2002**, *35*, 4725.

Table 1. Summary of Magnetic Alignment[a]

layered silicate		Epon 862	Epon 828	water	toluene	alignment to **H** field
I.30E (NC18)	NC	X	X		X	⊥
I.31PS		X	X			⊥
SC18	SC	X	X			∥
SC16		X				∥
SC14		X				∥
SC12		X				∥
Cloisite 6A		X			X	∥
Cloisite 20A		X				∥
Cloisite 30B		X				∥
Na MMT				X		∥

[a] The column heads for columns 2−6 indicate the matrix. Key: ⊥, perpendicular to **H**; ∥, parallel to **H**; NC, Nanocor; SC, Southern Clay. Empty fields indicate samples which have not been tried. Specifics for each montmorillonite are summarized in the Experimental Section.

interlayer cation, dispersion medium, and strength of the applied magnetic field (1.2 and 11.7 T). These imply that the different response to the applied magnetic field arises from the nonexchangeable portion of the MMT.

In a further experiment, equal quantities of powders of both MMTs were mixed in Epon 862/W to obtain a comparable 6 wt % nanocomposite. Both MMTs behaved independently within the magnetic field, yielding a four-point SAXS pattern after curing with *d* spacings and alignment consistent with those of the prior studies on the single-MMT systems. This reflects an orthogonal alignment of layers throughout the 5 mm by 50 mm rod with SC18 layers parallel to ($S_d = 0.51$) and NC18 layers perpendicular to ($S_d = -0.252$) the applied magnetic field. The two-dimensional nature of the layer results in a triaxially reinforcing microstructure with the orientational distribution of the long axis of the layer maximized along all three principal directions. Note that triaxial reinforcement is distinct from triaxial alignment, which can occur for rods but not plates as schematically summarized in Figure 2.

The magnetic response of smectites such as MMT is primarily determined by the concentration and distribution of paramagnetic ions within the aluminosilicate crystal structure. In natural MMT, 1−4% iron, mainly in the octahedral lattice positions and existing in two oxidation states, Fe(II) and Fe(III), leads to a paramagnetic response with the mass magnetic susceptibility $\chi \approx (1-5) \times 10^{-6}$ emu/(g Oe)[25−27] (MMT density $\rho \approx 2.5$ g/cm^3). Synthetic MMTs, which commonly lack iron, are diamagnetic ($\chi < 0$).[27] Note that Callaway and McAtee showed that the susceptibility does not directly correlate with the amount of Fe in the layered silicates[26] but may also be related to the presence of additional paramagnetic atoms in the lattice or separate phases (Mn^{2+}, Ti^{3+}) as well as the existence of paramagnetic centers intrinsic to the lattice (stable hole traps due to ionizing radiation or grinding). Schmidt-Rohr et al. also suggest that this may be due to small amounts of ferromagnetic components which have a large low-field

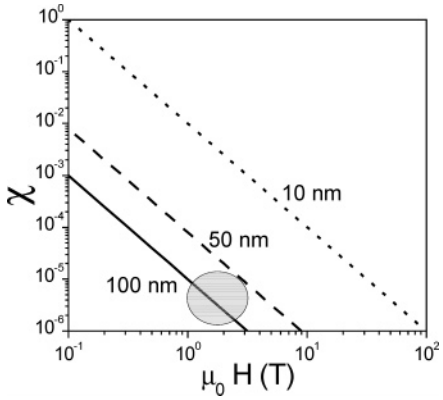

Figure 3. First-order calculations (Supporting Information) on the threshold external field necessary to overcome thermal randomization and induce deterministic alignment reveal that for volume magnetic susceptibilities comparable to that of MMT ($\kappa = \chi\rho \approx 10^{-5}$), magnetic fields between 1 and 3 T ($(1-3) \times 10^4$ G) are required.

susceptibility but saturate at intermediate fields.[27] Chemical analysis of the base MMTs used for organic modification indicate that the mean composition of a unit cell of SC is $(Si_{7.8}Al_{0.2}O_{16})(Al_{2.96}Fe_{0.45}Mg/Ca_{0.46}[]_{0.13}O_4(OH)_4)Na_{0.66}$ (CEC = 91 mequiv/100 g) and that of NC is $(Si_{7.72}Al_{0.28}O_{16})(Al_{2.7}Fe_{0.39}Mg/Ca_{0.91}[]_{0.13}O_4(OH)_4)Na_{1.19}$ (CEC = 145 mequiv/100 g).[28] The magnetic anisotropy determined above 50 K on macrocrystalline sheets of mica and vermiculate minerals indicates that the easy axis susceptibility is within the plane of the aluminosilicate sheet.[29] First-order calculations on the threshold external field necessary to overcome thermal randomization and induce deterministic alignment, Figure 3 and Supporting Information, reveal that, for volume magnetic susceptibilities comparable to that of MMT ($\kappa = \chi\rho \approx 10^{-5}$), magnetic fields between 1 and 3 T ($(1-3) \times 10^4$ G), readily available with rare-earth alloys (neodymium iron boron (NIB)), are sufficient to induce a response of paramagnetic particles with diameters of 70−100 nm. These factors are in agreement with the observed parallel alignment of the SC MMT with the applied magnetic field.

The paramagnetic response of MMTs though does not account for the opposite alignment of the NC MMT. Figure 4 summarizes superconducting vibrating sample magnetometer (VSM) data at 300 K for NC and SC. The magnetic mass susceptibility χ ($\chi_{NC} = 7.08$ emu/(g Oe) $\times 10^{-6}$, $\chi_{SC} = 6.12$ emu/(g Oe) $\times 10^{-6}$) is in good agreement with data reported in the literature.[25,27] However, the hysteresis, significantly more pronounced for NC, indicates the presence of antiferro- and ferrimagnetic phases in both MMTs and associated remnant magnetization $\mathbf{M}_F$ ($\mathbf{M}_{F,NC} = 0.0055$ emu/cm^3, $\mathbf{M}_{F,SC} = 0.0015$ emu/cm^3). Investigations at different temperatures show an increase in magnetization from 300 to 5 K as expected (Bloch's law) and a Curie temperature, T_C, for the majority antiferro/ferrimagnetic phase in both systems greater than 500 °C.

Antiferromagnetic impurities such as goethite (α-FeOOH; Néel temperatures $T_N \approx 130$ and 677 °C) and hematite (α-Fe_2O_3) and ferrimagnetic impurities such as magnetite (Fe_3O_4; Curie temperature $T_C \approx 585$ °C) are common within

(25) Hunt, C. P.; Moskowitz, B. M.; Banerjee, S. K. Magnetic Properties of Rocks and Minerals. In *Rock physics and phase relations: a handbook of physical constants*; Ahrens, T. J., Ed.; American Geophysical Union: Washington, DC, 1995; p 189.
(26) Callaway, W. S.; McAtee, J. L. *Am. Mineral.* **1985**, *70*, 996.
(27) Levin, E. M.; Hou, S. S.; Bud'ko, S. L.; Schmidt-Rohr, K. *J. Appl. Phys.* **2004**, *96*, 5085.
(28) Chemical formulas were calculated on the basis of chemical analysis obtained from Southern Clay and Nanocor.
(29) Ballet, O.; Coey, J. M. D. *Phys. Chem. Miner.* **1982**, *8*, 218.

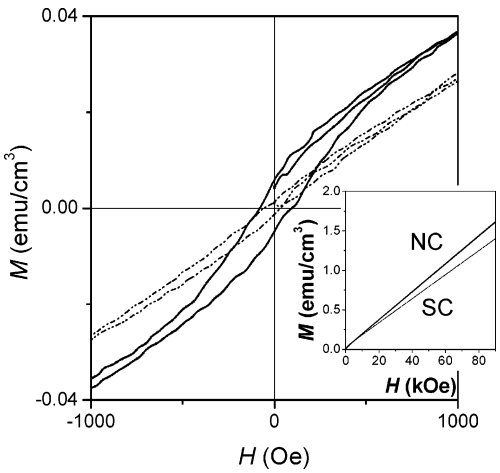

Figure 4. SC-VSM data of NC (solid) and SC (dashed) at 300 K showing hysteresis at $\mathbf{M} = \mathbf{H} = 0$. The remnant magnetization, $\mathbf{M}_F$ (intercept at $\mathbf{H} = 0$ of the linear extrapolation of the high-field magnetization curve), of NC is significantly larger than that of SC ($\mathbf{M}_{F,NC} = 0.0055$ emu/cm^3, $\mathbf{M}_{F,SC} = 0.0015$ emu/cm^3), indicative of a much larger contribution of antiferro- and/or ferrimagnetic components. The mass magnetic susceptibilities of the two systems are (SC) $\chi = \mathbf{M}/\mathbf{H} = 6.12$ emu/(g Oe) $\times 10^{-6}$) and (NC) $\chi = \mathbf{M}/\mathbf{H} = 7.08$ emu/(g Oe) $\times 10^{-6}$). The inset shows the paramagnetic response of **M** over the entire measured field of 9 T (90 kOe).

clay deposits where MMT is the majority mineral. These are commonly eliminated by extensive purification.[25] Small traces of isolated mineral impurities within these highly purified MMTs are possible, but unless they are intimately associated with the crystal structure of the aluminosilicate layers, they could not account for the global response of all the tactoids to the applied field. The observed magnetic response of NC, which is orthogonal to the easy axis susceptibility, must arise from (a) iron-rich impurities that are intimately associated with every one of the aluminosilicate tactoids, (b) local clustering of Fe within the aluminosilicate layer that is sufficient to lead to spin coupling, and/or (c) "impurities" or "defects" within the crystal lattice that alter the easy susceptibility axis of the layer. The first two possibilities could account for the observed hysteresis. The mean composition of a unit cell determined from chemical analysis does not exclude composition variations across an aluminosilicate layer. Composition changes of the growth medium during geological formation or alteration may produce local clustering of Fe impurities.[25] If clustering of Fe and associated antiferro/ferrimagnetic behavior is responsible for the observed alignment, the common magnetization direction with respect to the aluminosilicate layer must reflect the processing history or even the earth's magnetic field during deposition.[25] The exact nature of impurities or defects in MMTs is the subject of further investigation.

High-resolution transmission electron microscopy (HR-TEM) (50 nm thin microtomed films) of the mixture of SC18 and NC18 shown in Figure 5 verifies the global orthogonal alignment of the aluminosilicate layers and the anticipated ordered exfoliated morphology from the Epon 862/W system.[10] HRTEM of uniaxially aligned single-component nanocomposites show similar morphological features. The original tactoids are swollen, with spacing between layers ranging from 4 to >15 nm, and only a few individual, unassociated layers are observed. The low-magnification image (Figure 5a) and the accompanying digital Fourier transformation (Figure 5b) verify the overall orthogonal alignment of the epoxy-swollen tactoids in the mixed MMT system. At a higher magnification (Figure 5d,e), areas with oppositely aligned layers are visible. The DFT in Figure 5b shows *d* spacings of 10.2 nm (NC18) and 8.4 nm (SC18) in agreement with SAXS data (Figure 5c) of 10 nm (NC18) and 11 nm (SC18), indicating both techniques are sampling representative morphologies.[30]

The mechanical characteristics of the nanocomposites are impacted by the tailored morphology of the MMT. Figure 6 compares the CTEs at 6 wt % (3.7 vol %) MMT for the magnetically aligned morphologies, and contrasts them to those of random MMT morphologies. As expected, the addition of MMT leads to an overall decrease in CTE in the rubbery phase ($T > T_g$) ($T_g = 150$ °C). Note that the CTE of pure Epon 862/W at T/T_g varies between 450 and 500 ppm/°C[10] depending on the curing history and has been reported as high as 600 ppm/°C.[17] For the random morphologies, CTE decreases to approximately 375 ppm/°C. When aligned, the CTE further decreases along the reinforcement direction (SC18, parallel to the field **H**; NC18, perpendicular to **H**), whereas it increases in the orthogonal direction, reflecting the uniaxial orientation of the MMTs. The orthogonal arrangement of the SC18/NC18 mixture leads to CTEs at 340 ppm/°C, which is slightly lower than the average between the two individual extremes. Changes in the thermal or mechanical properties below T_g were within experimental error and are not displayed. For the Epon 862/W system used herein, the maximum impact on mechanical properties, especially within a glassy matrix, is compromised given the nonideal exfoliation. Reinforcement is by nanostructured "hybrid" particles, whose internal structure reflects that of the initial tactoid swollen by epoxy, and leads to compositional heterogeneities on the micrometer scale. As in conventional filled polymers, strain shielding, stress concentration, and inadequate stress transfer to the reinforcement phase are anticipated to compromise maximum performance.[3] More uniform dispersion of MMT in epoxy, by either extensive shear or B-staging through surface-initiated prepolymerization of the resin within a solvent, requires further development. Irrespective of these shortcomings, the three-dimensional reinforcement of two independently aligning layered silicates in an epoxy matrix leads to a significantly lower thermal coefficient of expansion.

In summary, magnetic fields >1 T can be used to align MMT in an epoxy matrix before curing. The penetration of magnetic fields through polymers implies that morphologies can be manipulated throughout bulk samples such as 5 × 50 mm rods demonstrated herein. The response arises from the aluminosilicate layer, implying the process is generally applicable as long as the field strength is sufficient to overcome the viscosity and drag of the medium. The uniaxial morphologies alter the thermal mechanical properties; however, further development of processing and predictable structure−property relationships are necessary to determine the maximum efficacy. There is a critical component of the

(30) Drummy, L.; Koerner, H.; Vaia, R. A. Manuscript in preparation.

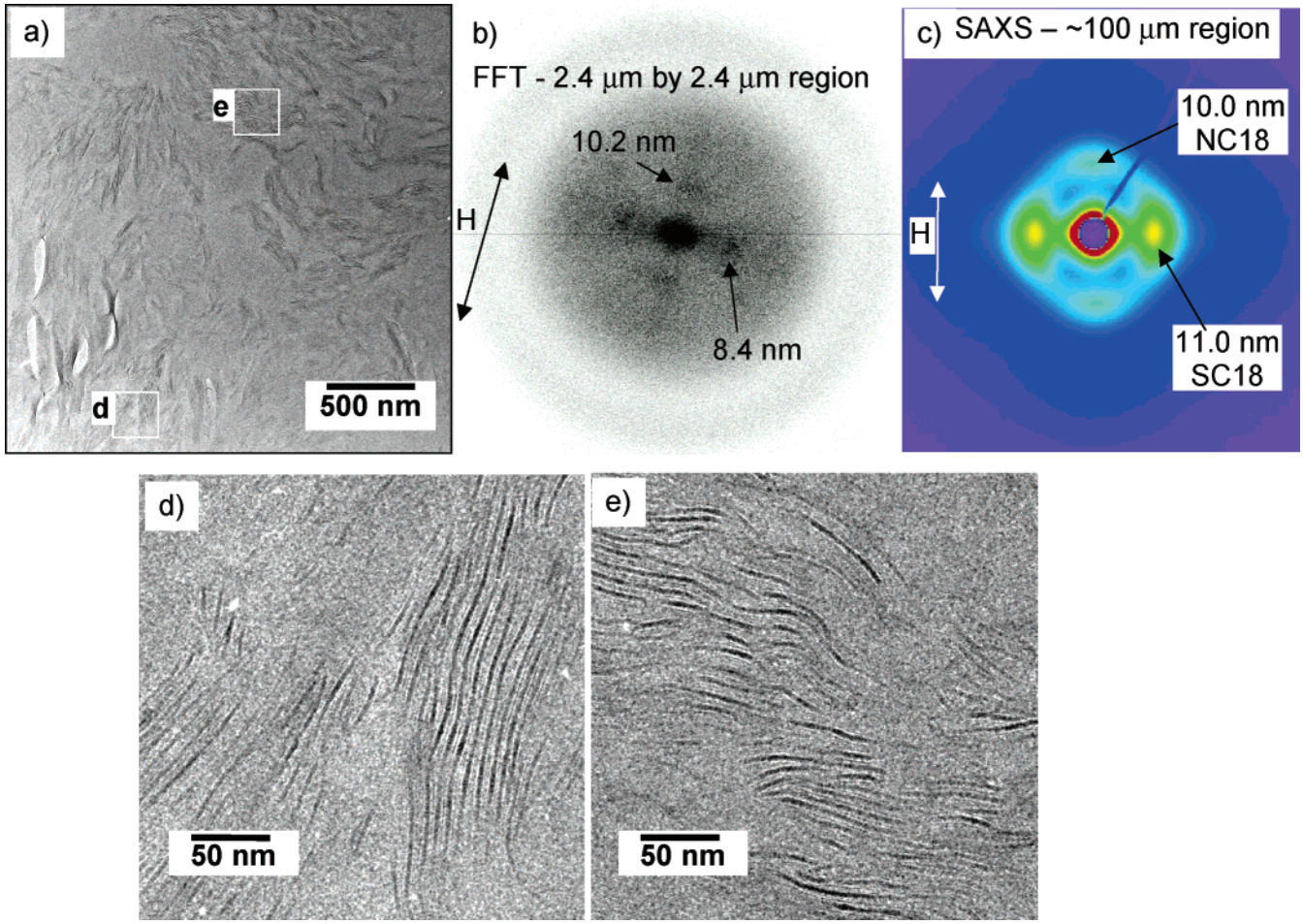

Figure 5. HRTEM of a 6 wt % mixture of SC18 and NC18: (a) low-magnification TEM showing orthogonal alignment of tactoids; (b) digital Fourier transformation (DFT) of the 2.4 × 2.4 μm area in (a) showing diffraction peaks arising from the independently aligned MMTs; (c) small-angle X-ray pattern showing a four-point pattern caused by orthogonally aligned MMT tactoids; (d) magnification of area d in (a) showing SC18 tactoids with parallel alignment; (e) magnification of area e in (a) showing NC18 tactoids with perpendicular alignment.

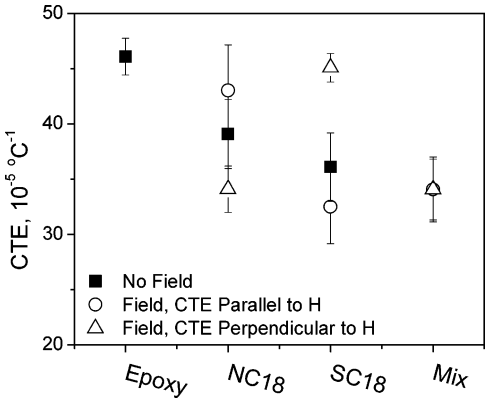

Figure 6. Coefficient of thermal expansion (CTE) within the rubbery region ($T > T_g \approx 150$ °C) of 6 wt % (3.7 vol %) MMT/epoxy nanocomposites aligned in a magnetic field (open) as well as comparable systems with random alignment of MMT (closed). Error bars show the standard deviation of five sample measurements.

chemistry in these nanofillers that has been overlooked in the past; small differences in chemical composition and chemical heterogeneities may allow researchers to explore many more possible techniques to address issues of nanocomposites. A remarkably minor compositional difference between MMTs can alter the effective susceptibility axis by 90°. Thus, by combining different MMTs, triaxial reinforcement of epoxy by the aluminosilicate layers is achievable. Overall, the magnetic susceptibility behavior of MMTs reinforces that they should not be considered simple homogeneous monoliths, but are compositionally complex heterogeneous crystals. As such, more detailed "inorganic" manipulation of the aluminosilicate layers, beyond altering surfactants via exchange reactions, has substantial potential to impart novel properties for both processing and performance.

Experimental Section

Nanocomposites were prepared using Nanocor I.30E (here referred to as NC18, 145 mequiv/100 g, octadecylammonium bromide, $\rho = 1.7$ g/cm^3, Nanocor[31]) and SC18, a Southern Clay Cloisite Na MMT (91 mequiv/100 g, $\rho \approx 1.9$ g/cm^3) modified with octadecylammonium chloride according to standard procedures.[16]

The thermoset matrix consisted of Epon 862 (bisphenol F epoxide) with diethyltoluenediamine (Epikure W, Resolution Performance Products) with a ratio of 100:26 (density $\rho \approx 1.03$ g/cm^3). The general fabrication procedure followed that reported by Chen et al.[17] In brief, the organically modified montmorillonite (OMM) was dispersed in the epoxy monomer with sonication and high shear mixing. After additional short mixing with curing agent W and subsequent degassing, the suspensions were filled into 5

(31) Company product information: G-105 polymer-grade montmorillonites, Nanocor, Inc.

mm NMR tubes for alignment in a magnetic field of 11.7 T (Oxford Instruments, Oxford, U.K.). A three-stage curing reaction (90 °C for 8 h, 120 °C for 2 h, 175 °C for 2 h) was used, where the initial stage was carried out within the NMR instrument (maximum temperature for NMR). Additional studies were conducted with a 1.2 T permanent magnet where the resin was filled into an X-ray capillary, placed with the magnetic field, alignment monitored in situ with X-ray scattering, and finally removed and cured (120 °C for 2 h and 175 °C for 2 h). Differential scanning calorimetry (TA Instruments Q1000) verified complete curing for these cure histories and all concentrations of OMM discussed.

In addition to the detailed systems discussed above, comparable alignment response to applied magnetic fields (1.2 T) has been observed for several other OMMs in Epon 862, Epon 828, water, and toluene (Table 1). Specifically, OMMs based on the Na+Montmorillonite PGV (NC, Nanocor, Inc.) include Nanocor I.28E (octadecylammonium bromide) and I.31PS (proprietary ammonium). OMMs based on Na+Montmorillonite Cloisite NA (SC, Southern Clay Products) include Cloisite 30B (methyl tallow bis-2-hydroylethylammonium; MER = 90), Cloisite 20A (dimethyl ditallow ammonium bromide; MER = 95), Cloisite 6A (dimethyl ditallow ammonium bromide; MER = 140), SC12 (dodecylammonium bromide; MER = 91), SC14 (tetradecylammonium bromide; MER = 91), and SC16 (hexadecylammonium bromide; MER = 91).

OMM morphologies were determined via X-ray diffraction and transmission electron microscopy. X-ray diffraction was conducted on Bruker AXS D8 Discover and Molecular Metrology SAXS instruments in transmission mode. Herman's orientation parameters were calculated according to standard procedures[32] from azimuthal integration of diffraction peaks. Ultrathin sections of the silicate/epoxy samples were cut using an RMC PowerTome XL ultramicrotome equipped with a Diatome diamond knife for TEM analysis. A cutting speed of 1 mm/s was used to cut 50 nm thick sections at room temperature. Sections were collected on 400 mesh copper grids. The sections were then coated with a thin layer (~10 nm) of amorphous carbon to improve the stability of the sections during electron irradiation. Microscopy was done on a Philips CM 200 operating at 200 kV. A CCD camera was used for focusing at high magnification. Images were collected on an SO-163 film and digitized using a Minolta DiMAGE scanner at 2400 dpi resolution.

Magnetic properties were investigated using a Quantum Design P252 VSM equipped with a 9 T superconducting magnet. Magnetic mass susceptibility was obtained from the slope **M**/**H** of the VSM data from 0.5 to 90 kOe. The bulk density of SC and NC is 2.5 g/cm^3. Data are given in cgs units for comparison with data reported in the literature.

Thermal mechanical measurements of the coefficient of thermal expansion were obtained with a TA Instruments 2940 TM analyzer at 4 °C/min. Reported values are the average of five samples, with error bars representing standard deviations.

Acknowledgment. We thank G. Price and M. Houtz (UDRI) for help with the X-ray and TMA experiments, Jennifer Brubaker for layered silicate modifications, Igors Sics at beamline X-27C of the National Synchrotron Light Source at Brookhaven for help with the time-resolved X-ray experiments, and Christi Vestal for fruitful discussions. L.D. is supported through the National Research Council Fellowship Program. The Air Force Office of Scientific Research, the Air Force Research Laboratory, and the Materials and Manufacturing Directorate provided funding.

Supporting Information Available: Text and figures describing the X-ray scattering studies of alignment and relaxation rate, and the threshold for deterministic motion within a magnetic field (PDF). This material is available free of charge via the Internet at http://pubs.acs.org.

CM048139M

(32) Koerner, H.; Luo, Y.; Li, X.; Cohen, C., Hedden, R. C.; Ober, C. K. *Macromolecules* **2003**, *36* (6), 1975.